



Excess enthalpy of mixing of mineral solid solutions derived from density-functional calculations

Artur Benisek¹ · Edgar Dachs¹

Received: 18 November 2019 / Accepted: 1 February 2020 / Published online: 17 February 2020
© The Author(s) 2020

Abstract

Calculations using the density-functional theory (DFT) in combination with the single defect method were carried out to determine the heat of mixing behaviour of mineral solid solution phases. The accuracy of this method was tested on the halite–sylvite (NaCl–KCl) binary, pyrope–grossular garnets ($\text{Mg}_3\text{Al}_2\text{Si}_3\text{O}_{12}$ – $\text{Ca}_3\text{Al}_2\text{Si}_3\text{O}_{12}$), MgO–CaO (halite structure) binary, and on Al/Si ordered alkali feldspars ($\text{NaAlSi}_3\text{O}_8$ – KAlSi_3O_8); as members for coupled substitutions, the diopside–jadeite pyroxenes ($\text{CaMgSi}_2\text{O}_6$ – $\text{NaAlSi}_2\text{O}_6$) and diopside–CaTs pyroxenes ($\text{CaMgSi}_2\text{O}_6$ – CaAlAlSiO_6) were chosen for testing and, as an application, the heat of mixing of the tremolite–glaucofane amphiboles ($\text{Ca}_2\text{Mg}_5\text{Si}_8\text{O}_{22}(\text{OH})_2$ – $\text{Na}_2\text{Mg}_3\text{Al}_2\text{Si}_8\text{O}_{22}(\text{OH})_2$) was computed. Six of these binaries were selected because of their experimentally well-known thermodynamic mixing behaviours. The comparison of the calculated heat of mixing data with calorimetric data showed good agreement for halite–sylvite, pyrope–grossular, and diopside–jadeite binaries and small differences for the Al/Si ordered alkali feldspar solid solution. In the case of the diopside–CaTs binary, the situation is more complex because CaTs is an endmember with disordered cation distributions. Good agreement with the experimental data could be, however, achieved assuming a reasonable disordered state. The calculated data for the Al/Si ordered alkali feldspars were applied to phase equilibrium calculations, i.e. calculating the Al/Si ordered alkali feldspar solvus. This solvus was then compared to the experimentally determined solvus finding good agreement. The solvus of the MgO–CaO binary was also constructed from DFT-based data and compared to the experimentally determined solvus, and the two were also in good agreement. Another application was the determination of the solvus in tremolite–glaucofane amphiboles ($\text{Ca}_2\text{Mg}_5\text{Si}_8\text{O}_{22}(\text{OH})_2$ – $\text{Na}_2\text{Mg}_3\text{Al}_2\text{Si}_8\text{O}_{22}(\text{OH})_2$). It was compared to solvi based on coexisting amphiboles found in eclogites and phase equilibrium experiments.

Keywords Thermodynamics · Heat of mixing · First principles · Ab initio · DFT · CASTEP · MgO–CaO · Halides · Garnets · Feldspars · Pyroxenes · Amphiboles

Introduction

This contribution is a continuation of our former study (Benisek and Dachs 2018), where we calculated internal energies and entropies of 21 well-known endmembers using the density-functional theory (DFT) and transformed them into standard enthalpies of formation from the elements and

standard entropies enabling a direct comparison with the measured quantities. These data were then integrated into existing thermodynamic data sets, making them available to a broad range of applications (Benisek and Dachs 2018). Since many mineral phases are solid solutions, thermodynamic mixing properties are essential for any petrologically relevant phase equilibrium calculations.

The enthalpy of a solid solution at a particular composition ($H_{(X)}$) may deviate from the behaviour of a mechanical mixture, i.e. from the linear combination of the enthalpies of the endmembers A and B (H^{mechmix}):

$$H^{\text{mechmix}} = (X_A H^A + X_B H^B). \quad (1)$$

H^A , H^B , X_A , and X_B are the enthalpies and the mole fractions of the A and B components, respectively. This

Electronic supplementary material The online version of this article (<https://doi.org/10.1007/s00269-020-01085-8>) contains supplementary material, which is available to authorized users.

✉ Artur Benisek
artur.benisek@sbg.ac.at

¹ Chemistry and Physics of Materials, University of Salzburg, Jakob-Haringer-Str. 2a, 5020 Salzburg, Austria

deviation is called the excess enthalpy of mixing or the heat of mixing (ΔH^{mix}):

$$\Delta H^{\text{mix}} = H_{(X)} - ((1 - X_B)H^A + X_B H^B). \quad (2)$$

ΔH^{mix} is a substantial thermodynamic property describing the behaviour of solid solutions. This property is responsible for ordering and exsolution phenomena, e.g. exsolution lamellae in feldspars (perthite), in calcite–dolomite and in pyroxene solid solutions; ordering in omphacite. ΔH^{mix} data can be measured experimentally by solution calorimetry (e.g. Navrotsky 1997; Hovis 2017; Benisek et al. 2003; Carpenter et al. 1985; Newton et al. 1977), which is a rather time-consuming technique. These data are then described by a mixing model using so-called interaction parameters (W_{AB} and W_{BA}), e.g. the Margules mixing model:

$$\Delta H^{\text{mix}} = (1 - X_B)X_B^2 W_{AB} + (1 - X_B)^2 X_B W_{BA}. \quad (3)$$

Such a description is necessary to define the activity–composition relations, which are then needed for petrological investigations (e.g. geothermometry, calculations of equilibrium phase diagrams).

However, ΔH^{mix} can also be calculated by ab initio methods (e.g. Ozolins et al. 1997). A particularly effective way of calculating ΔH^{mix} of a disordered phase at any intermediate composition is the single defect method of Sluiter and Kawazoe (2002). This method makes use of a single substitutional defect incorporated into a supercell of a host endmember. The energy calculations for the endmembers and for such supercells provide direct knowledge of the interaction parameters, because the results can be easily transformed into the slopes of the heat of mixing functions in the limits of $X_B = 0$ and $X_B = 1$ (Li et al. 2014). The ΔH^{mix} calculated by the single defect method represents that of a disordered solid solution as discussed by many studies (e.g. Vinograd and Sluiter 2006; Vinograd and Winkler 2010; Vinograd et al. 2013; Li et al. 2014; Vinograd et al. 2018).

In this study, the single defect method was tested on the following solid solutions: halite–sylvite (NaCl–KCl), pyrope–grossular ($\text{Mg}_3\text{Al}_2\text{Si}_3\text{O}_{12}$ – $\text{Ca}_3\text{Al}_2\text{Si}_3\text{O}_{12}$), MgO–CaO (with halite structure), Al/Si ordered alkali feldspar ($\text{NaAlSi}_3\text{O}_8$ – KAlSi_3O_8), and two binaries characterised by coupled substitutions, i.e. diopside–jadeite pyroxenes ($\text{CaMgSi}_2\text{O}_6$ – $\text{NaAlSi}_2\text{O}_6$) and diopside–CaTs pyroxene ($\text{CaMgSi}_2\text{O}_6$ – CaAlAlSiO_6).

These six binaries were chosen because their thermodynamic mixing behaviours are well known from calorimetric or phase equilibrium experiments, enabling a direct comparison of calculated with experimentally derived mixing behaviours and thus an assessment if DFT in combination with the single defect method can provide reasonable results. The enthalpic mixing behaviour of the halite–sylvite

binary was investigated by solution calorimetry at 298 K in the work of Barrett and Wallace (1954) and that of the pyrope–grossular binary by high-temperature solution calorimetry (Newton et al. 1977). ΔH^{mix} of the alkali feldspar binary studied by Hovis (1988) was reinvestigated in 2017 by HF solution calorimetry by the same author on a large number of specimens producing well-defined heat of Na–K mixing data (Hovis 2017). ΔH^{mix} of the diopside–jadeite binary was measured by high-temperature solution calorimetry (Wood et al. 1980). The same method was used to measure ΔH^{mix} of the diopside–CaTs solid solution by Newton et al. (1977) and reinvestigated by Benisek et al. in 2007, who found results consistent with those of the former study.

The calculated ΔH^{mix} of the Al/Si ordered alkali feldspar binary in combination with measured vibrational entropy of mixing data ($\Delta S_{\text{vib}}^{\text{exc}}$) was then applied to calculate the corresponding solvus, allowing a comparison with the one studied experimentally by the ion exchange and homogenisation–unmixing techniques (Bachinski and Müller 1971). A more sophisticated procedure that calculated both ΔH^{mix} and $\Delta S_{\text{vib}}^{\text{exc}}$ using DFT methods was applied to the MgO–CaO binary. The solvus in this join was determined independently by many researchers (e.g. Doman et al. 1963) via phase equilibrium experiments, all of which were modelled by Yin and Argent (1993). As an application of determining ΔH^{mix} of a binary for which no calorimetric data exist, tremolite–glaucophane amphiboles were chosen. The resulting data, together with estimated entropy data, were used to construct the solvus and to compare it with solvi obtained from naturally coexisting amphiboles found in different eclogites (Reynard and Ballevre 1988) and from phase equilibrium experiments (Jenkins et al. 2014).

Experimental methods

Computational methods

Quantum mechanical calculations were based on the DFT plane wave pseudopotential approach implemented in the CASTEP code (Clark et al. 2005) included in the Materials Studio software from Biovia®. The calculations used the local density approximation (LDA) for the exchange–correlation functional (Ceperley and Alder 1980) and norm-conserving pseudopotentials to describe the core–valence interactions. For the k-point sampling of the investigated unit cells, a Monkhorst–Pack grid (spacing of 0.03/Å) was used (Monkhorst and Pack 1976) and convergence was tested by performing calculations using a denser k-point grid. The structural relaxation was calculated by applying the BFGS algorithm (Pfrommer et al. 1997), where the convergence threshold for the force on an atom was 0.01 eV/Å. In addition to the LDA calculations, the gradient corrected

functional (GGA-PBE, Perdew et al. 1996) and its revised form for solids (GGA-PBESOL, Perdew et al. 2008) were used in some cases.

Single defect method to calculate the heat of mixing (ΔH^{mix})

In a first step, the internal energies (E) of the unit cells of the endmembers were calculated and normalised to one formula unit. Next, large supercells were generated containing one single substitutional defect. In the case of the pyrope–grossular solid solution, for example, the largest supercell contained 47 Ca plus 1 Mg on the dodecahedral positions, which is equal to the size of 16 formula units and a mole fraction of $X_{\text{Gr}} = 47/48$. Other supercells of this binary contained 23 Mg plus 1 Ca and 23 Ca plus 1 Mg on the dodecahedral positions, resulting in mole fractions of $X_{\text{Gr}} = 1/24$ and $23/24$, respectively. The internal energies of these supercells were then calculated and normalised to one formula unit. The excess internal energy of mixing (ΔE^{mix}), i.e. the deviation from the linear combination of the internal energies of the endmembers, was calculated according to Eq. 2.

ΔE^{mix} and ΔH^{mix} are related by the volume term $P \Delta V^{\text{mix}}$. ΔV^{mix} is typically less than 1 J/bar/mol (e.g. Geiger 2001), whereas ΔE^{mix} is in the range of several kJ/mol. At a pressure of 1 bar, where the calculated ΔE^{mix} is compared to the measured ΔH^{mix} , the volume term $P \Delta V^{\text{mix}}$ can be neglected, i.e.

$$\Delta E^{\text{mix}} \approx \Delta H^{\text{mix}}. \quad (4)$$

DFT calculations of the vibrational excess entropy of mixing ($\Delta S_{\text{vib}}^{\text{exc}}$)

The vibrational excess entropy of mixing ($\Delta S_{\text{vib}}^{\text{exc}}$) is defined as the deviation from the linear combination of the vibrational entropies of the endmembers (similar to ΔH^{mix} , see Eq. 2). To calculate $\Delta S_{\text{vib}}^{\text{exc}}$ of a solid solution by DFT methods, investigations of large enough cells are necessary, as shown on Cu_3Au by Benisek et al. (2018). Otherwise, the results depend too strongly on the used atomic configuration. This situation occurred with Cu_3Au when investigating cells with only eight crystallographic sites on which substitutions took place. To simulate the random character of a solid solution, cells with 32 sites on which substitutions took place were necessary (Benisek et al. 2018).

Calculation of the solvus from DFT data

To model the solvus from thermodynamic data, the heat of mixing, ΔH^{mix} , the excess vibrational entropy of mixing, $\Delta S_{\text{vib}}^{\text{exc}}$, and the configurational entropy, S^{config} , have

to be known (e.g. Benisek and Dachs 2013; Benisek et al. 2014). Whereas ΔH^{mix} and $\Delta S_{\text{vib}}^{\text{exc}}$ can be calculated directly using DFT methods, the calculation of the excess configurational entropy (i.e. the deviation from the fully disordered state due to short-range ordering—SRO) would need additional methods, e.g. the cluster expansion method (Vinograd et al. 2009; Vinograd and Winkler 2010), which was not applied in this work. An estimate of the configurational excess entropy is nevertheless possible by comparing experimentally derived T – X positions of solvi (with samples that are characterised by SRO) with those calculated using DFT derived thermodynamic data (valid for the fully disordered state).

The T – X position of a solvus is calculated by finding those two compositions, for a given temperature and pressure, at which the chemical potentials of components A and B in the two coexisting phases, ph1 and ph2, forming the miscibility gap, are equal:

$$\mu_{\text{A}}^{\text{ph1}} = \mu_{\text{A}}^{\text{ph2}} \quad \text{and} \quad (5)$$

$$\mu_{\text{B}}^{\text{ph1}} = \mu_{\text{B}}^{\text{ph2}}. \quad (6)$$

Results and discussion

Halite–sylvite binary

In the halite–sylvite (NaCl – KCl) solid solution, Na and K are octahedrally coordinated by Cl atoms. To model the solid solutions, two large supercells containing 31 Na and 1 K on the Na-rich side and 31 K and 1 Na on the K-rich side were constructed. The cells had 32 formula units (FU) and mole fractions of $X_{\text{KCl}} = 1/32$ and $31/32$, respectively. The resulting ΔH^{mix} data were fitted to a Margules mixing model enabling a comparison with the measured data. As illustrated in Fig. 1, the calculated ΔH^{mix} values agree well with the experimental values. Very small deviations between calculated and measured ΔH^{mix} values can be found in the intermediate part of the solid solution. Here, experimental difficulties occur in producing samples without exsolutions (Barrett and Wallace 1954). Principally, the calculated ΔH^{mix} values depend on the size of the supercells. We, therefore, investigated additionally smaller supercells with only 8 FU and larger supercells with 108 FU. These data are presented in the supplementary materials (Supplementary Appendix A) and show that the single defects should be separated by a distance of at least ca. 12 Å (single defects of neighbouring cells), which is the case for supercells containing 32 FU. The supercells with

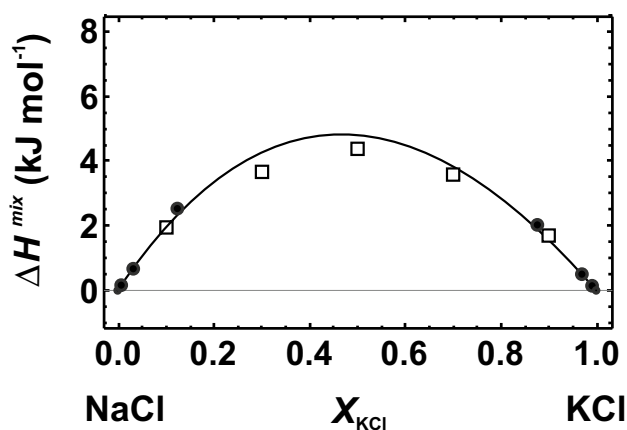


Fig. 1 Heat of mixing (ΔH^{mix}) of the halite (NaCl)–sylvite (KCl) binary. Experimental data from Barrett and Wallace (1954) are indicated by open squares. Their experimental errors (1 sd) are smaller than plot symbols. Closed circles represent the results from LDA calculations. The results using large supercells at $X_{\text{KCl}} \approx 0.03$ and 0.97 were fitted by a Margules mixing model (solid line). The LDA results from smaller and larger supercells are also shown

only 8 FU are characterised by distances between the single defects of ca. 8 Å. They produced significantly higher ΔH^{mix} values compared to the larger supercells.

The NaCl–KCl binary is characterised by positive vibrational excess entropies as measured by calorimetry by Benisek and Dachs (2013). Using these data, the Gibbs free energy of mixing and in consequence the halite–sylvite solvus were calculated showing good agreement with literature data (Barrett and Wallace 1954; Vesnin and Zakovryashin 1979). A comparison is given in the supplementary materials (Supplementary Appendix B).

Pyrope–grossular solid solution

This binary is characterised by Mg–Ca mixing on one crystallographic position, the dodecahedral site. The single defect method using the LDA functional yielded ΔH^{mix} values in good agreement with the calorimetric data of Newton et al. (1977) as presented in Fig. 2. In addition to the LDA calculations, the gradient-corrected functional (GGA-PBE, Perdew et al. 1996) and its revised form for solids (GGA-PBESOL, Perdew et al. 2008) were used to calculate ΔH^{mix} of this solid solution. The GGA-PBE functional provided results that are larger than the calorimetric ΔH^{mix} values, especially in the Ca-rich region (broken line in Fig. 2). In Fig. 2, additional results (using LDA and GGA-PBESOL, but not the single defect method) are shown, obtained from cells with intermediate compositions, each having different Ca/Mg configurations demonstrating that the resulting ΔH^{mix} values of such cells depend strongly on the configuration used. The LDA and GGA-PBESOL functionals resulted in similar ΔH^{mix} values.

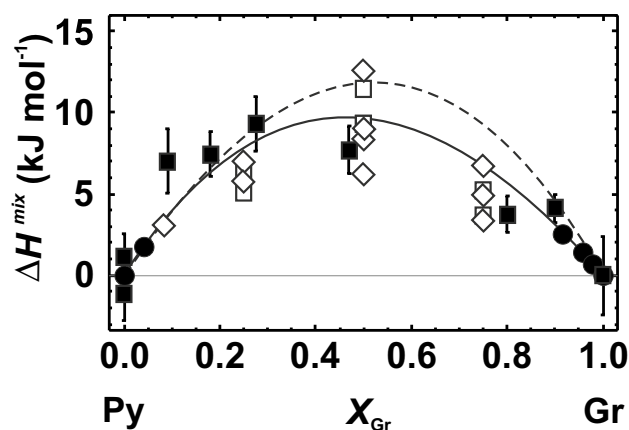


Fig. 2 Heat of mixing (ΔH^{mix}) of the pyrope (Py)–grossular (Gr) solid solution. Experimental data from Newton et al. (1977) are indicated by solid squares with error bars (1 sd). Closed circles represent ΔH^{mix} from LDA calculations using the single defect method and are modelled applying a Margules mixing model (solid line). Broken line shows the Margules fit to the results of GGA-PBE calculations (single defect). Open squares and diamonds: ΔH^{mix} derived from GGA-PBESOL and LDA calculations that are not based on the single defect method, but use different configurations in cells with intermediate composition

The ΔH^{mix} function using the LDA calculations (solid line in Fig. 2) is comparable to the results obtained by a cluster expansion method of Sluiter et al. (2004). The theoretical study of Vinograd and Sluiter (2006) proposed a temperature-dependent ΔH^{mix} behaviour for the pyrope–grossular solid solution. The ΔH^{mix} values at low temperatures (< 700 K) are significantly smaller than our LDA single defect results and those of Newton et al. (1977), but agree well at higher temperatures (~ 1500 K). At such high temperatures, the configurational entropy is that of a disordered solid solution (Vinograd and Sluiter 2006). The agreement of the ΔH^{mix} behaviour resulting from the single defect method with its high-temperature behaviour, as determined by Vinograd and Sluiter (2006), indicates that the single defect method yields ΔH^{mix} of a disordered solid solution.

MgO–CaO solid solution

The MgO–CaO binary has a halite structure, where Mg and Ca are octahedrally coordinated by oxygen atoms. To the best of our knowledge, no heat of mixing data exist for this solid solution. However, many experimentally determined solvus data have been published for this binary, which were compiled and recalculated by Yin and Argent (1993). We therefore performed DFT calculations for both ΔH^{mix} and $\Delta S_{\text{vib}}^{\text{exc}}$ to model the MgO–CaO solvus.

The results of the calculations with regard to enthalpy were described by a Margules mixing model using the interaction parameters $W_{\text{MgCa}}^H = 65.24$ and $W_{\text{CaMg}}^H = 86.83$ kJ/

mol. For the calculations of $\Delta S_{\text{vib}}^{\text{exc}}$, three cells with 64 atoms (24 Mg, 8 Ca, and 32 O) were investigated, differing in their atomic arrangements (disordered, clustered, or short-range ordered). All cells yielded almost identical results in accordance with the findings on Cu_3Au (Benisek et al. 2018). Applying calorimetry and DFT calculations, these authors showed that the vibrational entropy did not depend on the degree of short-range ordering in Cu_3Au . The latter method, however, requires the investigation of large enough cells containing at least 32 sites on which the substitution takes place. The independence of the vibrational entropy from the degree of short-range ordering may be explained by the following considerations: The geometry of distinct crystallographic sites, on which the substitution occurs, varies slightly from one site to the other in a disordered phase depending on the environment of the particular site. In a short-range ordered phase, there are sites where the environment of atom A is enriched with atom B (with different degrees of enrichment from one site to the other). The enthalpy and the configurational entropy of such short-range ordered structure differs from that of a fully disordered one. However, the phonons only see averaged crystallographic sites and hence the vibrational entropy tends to be independent of the degree of short-range ordering/clustering. This situation can be modelled in DFT calculations, if large enough cells are used in computing the dynamical matrix (Benisek et al. 2018). The resulting $\Delta S_{\text{vib}}^{\text{exc}}$ values for the MgO–CaO binary were described using a Margules model yielding $W_{\text{vib}}^{\text{S}} = 10.8 \text{ J/mol/K}$.

Using the obtained mixing parameters, a solvus can be calculated and compared with the experimentally determined solvus. The calculated solvus is at slightly too low temperatures (Fig. 3). As found for the NaCl–KCl binary (Benisek and Dachs 2013) and for the alkali feldspar solid solutions (Benisek et al. 2014), samples equilibrated at the P – T – X conditions of the solvi are characterised by SRO. This situation, however, may be better described by short-range clustering; i.e. the environment of a Na atom is enriched in Na atoms, and that of a K atom is enriched in K atoms. Such an atomic distribution should be expected near the point where exsolution textures are developed. This short-range clustering reduces the configurational entropy from that of a fully disordered solid solution crystal. In the case of the NaCl–KCl binary, the decrease in the configurational entropy due to short-range clustering was described by an asymmetric Margules mixing model using $W_{\text{NaK}}^{\text{S}} = 0$ and $W_{\text{KNa}}^{\text{S}} = -3 \text{ J/mol/K}$ (Benisek and Dachs 2013). In the case of the Al/Si disordered alkali feldspars, the decrease in the configurational entropy yielded $W_{\text{NaK}}^{\text{S}} = 0$ and $W_{\text{KNa}}^{\text{S}} = -7 \text{ J/mol/K}$ (Benisek et al. 2014).

The experimentally determined MgO–CaO solvus can be perfectly reproduced, if the configurational entropy of a disordered atomic distribution is reduced by an amount given

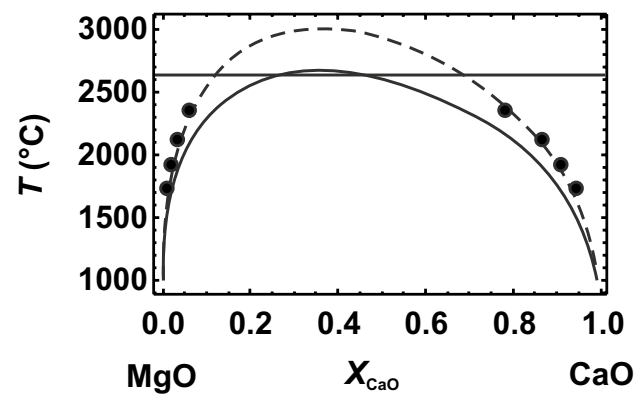


Fig. 3 DFT-based solvus (solid line) of the MgO–CaO system (halite structure) at 1 bar compared to the experimentally determined solvus (solid circles) of Yin and Argent (1993). The broken line represents a calculated solvus using the same DFT data (ΔH^{mix} and $\Delta S_{\text{vib}}^{\text{exc}}$) plus a small reduction of the configurational entropy due to possible short-range clustering. At 2630 °C, this system is characterised by the eutectic interactions and are not shown in detail

by a Margules mixing model with $W_{\text{MgCa}}^{\text{S}} = -2.5$ and $W_{\text{CaMg}}^{\text{S}} = -3 \text{ J/mol/K}$ (Fig. 3). These are quite realistic values and comparable to the situation in the NaCl–KCl and in the Al/Si disordered alkali feldspar solid solutions.

The vibrational entropy of the MgO–CaO solid solution was also calculated using a cell with only eight atoms (3 Mg, 1 Ca, and 4 O). The $\Delta S_{\text{vib}}^{\text{exc}}$ value of this particular cell was more than twice as much as that of the cell with 64 atoms, emphasising the need for large cells in simulating the vibrational entropy of solid solutions.

Al/Si ordered alkali feldspar solid solution

In alkali feldspars, Na–K mixing takes place on one crystallographic site, the irregular cavities in the tetrahedral framework. The DFT-based ΔH^{mix} data for Na–K mixing in Al/Si ordered feldspars are shown in Fig. 4, where they are compared to results from thoroughly investigated samples using HF calorimetry (Hovis 2017). The single defect DFT results are slightly lower than those of the calorimetric data, especially in the Na-rich region. In Fig. 4, additional results are shown (data in the intermediate compositional region, computed without using the single defect method). As was the case with the data for the pyrope–grossular binary, such an approach yields ΔH^{mix} values that depend strongly on the chosen configuration causing a scatter of 2–3 kJ/mol in ΔH^{mix} .

Using a Margules mixing model for the vibrational entropy with $W_{\text{vib}}^{\text{S}} = 9.1 \text{ J/mol/K}$, which is based on calorimetrically measured $\Delta S_{\text{vib}}^{\text{exc}}$ values (Benisek et al. 2014), the solvus for this binary was calculated by using either the calorimetric or the DFT-based ΔH^{mix} data. In Fig. 5, both solvi are shown allowing comparison to the experimentally

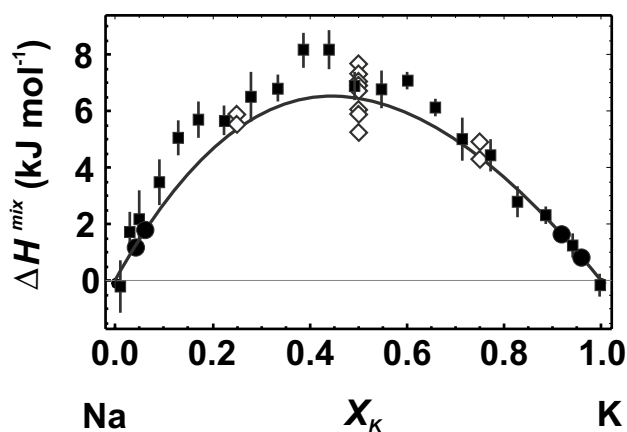


Fig. 4 Heat of mixing (ΔH^{mix}) of the low albite (Na)–microcline (K) binary. The experimental data of Hovis (2017) are shown by solid squares with error bars (1 sd). Closed circles and solid line show the results from DFT calculations using the single defect method. Open diamonds represent results from DFT calculations using cells with different Na–K configurations

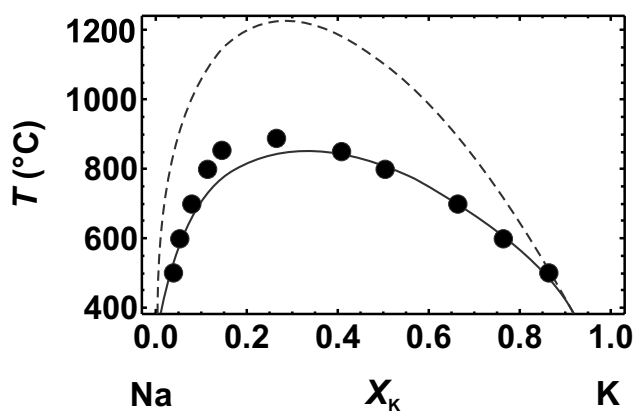


Fig. 5 Solvus of the Al/Si ordered alkali feldspar binary, low albite (Na)–microcline (K), at 1 bar. Solid circles show mean solvus data experimentally determined by Bachinski and Müller (1971). Solid line shows the miscibility gap calculated using ΔH^{mix} derived from the single defect method of this study. Broken line represents the solvus using ΔH^{mix} from Hovis (2017). In both cases, the behaviour of the vibrational entropy of mixing was calculated using an interaction parameter of $W^{\text{S}}=9.1$ J/mol/K (Benisek et al. 2014), which agrees with that of Haselton et al. (1983). The volume–composition behaviour does not play any role at 1 bar and is not considered

determined solvus of Bachinski and Müller (1971). The solvus calculated with DFT-based ΔH^{mix} has a slightly lower critical temperature than the experimentally determined solvus. Similar behaviour was found in the NaCl–KCl (Benisek and Dachs 2013), the Al/Si disordered alkali feldspar (Benisek et al. 2014), and the MgO–CaO binaries (this study). The difference for the Al/Si ordered alkali feldspar system is, though, small compared to those for the other binaries. Nevertheless, all binaries studied in this way (i.e.

comparing solvi that are based on ΔH^{mix} and $\Delta S_{\text{vib}}^{\text{exc}}$ values with experimentally determined ones) show similar characteristics, specifically, the need for excess configurational entropies to obtain agreement. The excess configurational entropies can be logically traced back to short-range clustering present in samples lying on the solvus. Such short-range clustering can be modelled using the configurational entropy of a fully disordered state plus a Margules mixing model using negative interaction parameters to describe the excess configurational entropy.

The calorimetrically based solvus of the Al/Si ordered alkali feldspars is, on the other hand, positioned at considerably higher temperatures than the experimentally determined solvus (Fig. 5). Positive excess configurational entropies would be required to achieve agreement, which is, however, not easy to explain. Hovis (2017) provided some explanations for such excess configurational entropies possibly present in his samples. At this point, note also that the solvus temperatures respond very sensitively to small changes in ΔH^{mix} . The differences between calorimetric and DFT-based ΔH^{mix} data are only ~ 1 kJ/mol, but produce solvi that differ by almost 400 °C. Small structural changes in the samples can thus change the solvus temperatures significantly. Hovis (2017) corrected his ΔH^{mix} values for small changes in the Al/Si distributions that occurred during homogenisation. Such a correction was, however, not applied by Bachinski and Müller (1971) to their samples. If these were characterised by Al/Si distributions that were not fully ordered, the correct solvus of the Al/Si ordered alkali feldspars would be higher.

Diopside–jadeite solid solution

The diopside–jadeite binary is characterised by the coupled substitution



where Ca is replaced by Na on the M2 site and Mg is replaced by Al on the M1 site, complicating the application of the single defect method. Strictly speaking, the single defect becomes a double defect. A previous study found that ΔH^{mix} of coupled substitutions depends on the defect combinations, i.e. on the distance between the two coupled defects. Such dependence was demonstrated for the Mg–Al biotites (Dachs and Benisek 2019) and is similarly expected for the pyroxene structure. The diopside structure has several possibilities for arranging the Na defect around the Al defect. There are three defect combinations with a distance of ~ 3.3 Å between them, two possibilities with a distance of 4.7 Å and many defect combinations with a distance of ~ 6 Å. If the distance between the defects on the M1 and M2 sites is smallest (first next nearest M1–M2 defect

combinations), ΔH^{mix} is slightly smaller than the calorimetric results from Wood et al. (1980). This difference is shown in Fig. 6, where the solid line represents the results from the first next nearest defect combinations, which can be modelled with $W^H = 27.98$ kJ/mol. If defect combinations with larger distances between them are also considered, ΔH^{mix} becomes increasingly larger. The dashed line in Fig. 6 represents the mean of five defect combinations ($W^H = 32.16$ kJ/mol) and agrees perfectly with the calorimetric results.

To estimate the configurational entropy arising from the different numbers of defect combinations, we calculated the jadeite activity (a_{Jd}) and compared it with the results of phase equilibrium experiments by Gasparik (1985), who studied the compositions of diopside–jadeite pyroxene in equilibrium with albite and quartz at 1200–1350 °C. The calculation of the activity of a component requires knowledge of ΔH^{mix} , $\Delta S_{\text{vib}}^{\text{exc}}$, and the deviation of the configurational entropy from that of a fully disordered state. To obtain $\Delta S_{\text{vib}}^{\text{exc}}$, we applied the estimation method of Benisek and Dachs (2012) because DFT calculations for cells including enough crystallographic sites on which the substitutions take place would be a very time-consuming task for this binary. We obtained a maximum $\Delta S_{\text{vib}}^{\text{exc}} = 0.64$ J/mol/K, which corresponds with a $W_{\text{vib}}^S = 2.54$ J/mol/K. Using these vibrational properties, the enthalpic excess quantities of the dashed line ($W^H = 32.16$ kJ/mol, Fig. 6) and an ideal activity of $a^{\text{id}} = X$ (mixing on one site; in the case of a coupled substitution this corresponds with molecular mixing), it turns out that positive excess configurational entropies given by $W_{\text{config}}^S = 21$ J/mol/K are

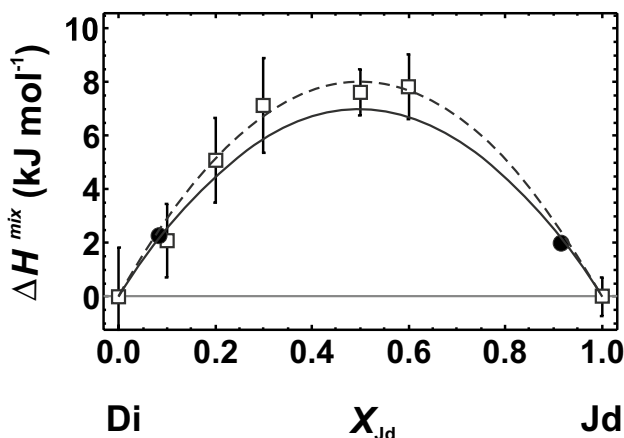


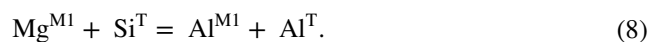
Fig. 6 Heat of mixing (ΔH^{mix}) of the diopside (Di)–jadeite (Jd) solid solution. Experimental data from Wood et al. (1980) are indicated by open squares with error bars (1 sd). Closed circles and solid line are from LDA calculations (single defect method), where the distance between defects on M1 and M2 sites is smallest (first next nearest M1–M2 defect pair). If defect combinations with larger distances between them are considered, ΔH^{mix} is increased. Broken line represents ΔH^{mix} resulting from the mean of the five next nearest defect combinations

needed to achieve good agreement with the phase equilibrium experiments by Gasparik (1985). These positive excess configurational entropies have a maximum value at $X_{\text{Jd}} = 0.5$ of $S^{\text{exc}} = 5.25$ J/mol/K. This value almost corresponds to a configurational entropy value of an additional site. Ideal mixing on one site produces a configurational entropy of $S^{\text{cfg}} = 5.76$ J/mol/K ($-R(X_A \times \ln(X_A) + X_B \times \ln(X_B))$) at maximum (at $X_A = X_B = 0.5$). This result means that the structural situation with five defect combinations corresponds with two almost independent crystallographic sites.

As already mentioned, the DFT calculations with five defect combinations agree well with the enthalpic behaviour of the samples from Wood et al. (1980). Most of these samples were synthesised at a temperature of 1350 °C. At lower temperatures, it can be expected that only the defect combinations with the smallest distances may be present in such crystals (enthalpic behaviour of the solid line in Fig. 6). The above comparison was therefore repeated using $W^H = 27.98$ kJ/mol, yielding an excess configurational entropy of $W_{\text{config}}^S = 18$ J/mol/K. Now, the maximum value of the excess configurational entropy is $S^{\text{exc}} = 4.5$ J/mol/K, considerably smaller than the configurational entropy of an additional site. This demonstrates that short-range ordering exists in the diopside–jadeite solid solution at temperatures between 900 and 1350 °C. At still lower temperatures, long-range ordering occurs in crystals with compositions around $\text{Di}_{50}\text{Jd}_{50}$, generating the $\text{C2/c} \rightarrow \text{P2/n}$ phase transition of the omphacites (e.g. Fleet et al. 1978). The results of the static lattice energy calculations of Vinograd et al. (2007) agree well with our calculations, showing that short-range ordering is relevant between ca. 900 and 1300 °C (their Fig. 5).

Diopside–CaTs solid solution

The diopside–Ca-Tschermak pyroxenes are another example of a binary characterised by a coupled substitution, i.e.



Here, M1 and the tetrahedral site T are involved in the substitution. The tetrahedral site of the endmember CaTs (CaAlAlSiO_6) is occupied by equal numbers of Al and Si. The two atoms are distributed somehow over one crystallographic site, implicating that CaTs is a disordered endmember. We first constructed a CaTs unit cell with alternating Al and Si on the tetrahedral chain (T–O–T); i.e. no Al–O–Al linkages were present within the tetrahedral chain. On the basis of this endmember, the resulting ΔH^{mix} values were large compared to measured data (Fig. 7). In a second approach, unit cells for CaTs were constructed that contained Al–O–Al linkages within the tetrahedral chain. One unit cell contained, for example, 4 Al–O–Al out of 32 T–O–T linkages to simulate a partly disordered CaTs structure. On the

basis of this endmember, a supercell with a single defect was constructed, thereby removing one Al–O–Al linkage due to the insertion of Si instead of Al. Such an approach yielded perfect agreement with the measured ΔH^{mix} behaviour (Fig. 7). Other disordered CaTs structures were also investigated, and they showed that a partly disordered structure yielded the best agreement with the calorimetric observations.

The CaTs samples in the calorimetric studies were synthesised at temperatures between 1523 and 1673 K. Similar samples were investigated by ^{29}Si MAS NMR spectroscopy (Cohen 1985; Bosenick et al. 1999; Flemming and Luth 2002), which revealed that such CaTs samples are characterised by a partly disordered Al/Si distribution on the tetrahedral site. In detail, they found that there were approximately 0.18 Al–O–Al linkages per formula unit (pfu). A fully disordered CaTs endmember would have 0.5 tetrahedral Al–O–Al, Al–O–Si, Si–O–Al, and Si–O–Si linkages pfu.

These observations are in very good agreement with our results; i.e. the CaTs structure with 4 Al–O–Al out of 32 T–O–T linkages yields the best agreement with the experimental observations. Such disordered cells contain a

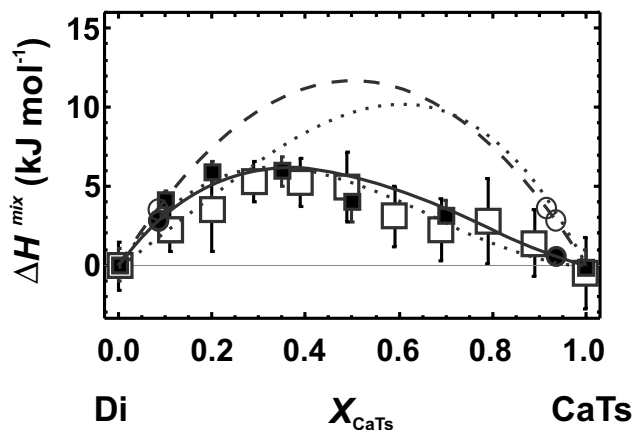


Fig. 7 Heat of mixing (ΔH^{mix}) of the diopside (Di)–Ca-Tschemmak (CaTs) solid solution. Experimental data from Benisek et al. (2007) and Newton et al. (1977), which are marked by open and closed squares with error bars, respectively (error bars represent 1 sd). Open circles and broken line represent the LDA results using the single defect method and an ordered CaTs endmember (without Al–O–Al bonds). Solid line and closed circles represent the LDA results using a partly disordered CaTs endmember (including 4 Al–O–Al linkages out of a total of 32 tetrahedral cation–anion–cation linkages, T–O–T). The CaTs-rich supercell was then constructed by inserting a substitutional defect into this partly disordered CaTs endmember, thereby reducing one Al–O–Al linkage. The dotted lines represent LDA results using other disordered CaTs endmembers. The upper dotted line shows the results, where CaTs had 8 Al–O–Al linkages out of 32 T–O–T (fully disordered) and the lower dotted line those using CaTs with 2 Al–O–Al out of 32 T–O–T. In both experiments, the CaTs-rich supercells are reduced by 1 Al–O–Al linkage through the insertion of the substitutional defect

ratio of 0.125 Al–O–Al linkages, which corresponds to 0.25 Al–O–Al linkages pfu (because there are two T–O–T linkages in one formula unit).

The calculations showed, however, that it is not possible to ascertain the ΔH^{mix} behaviour unequivocally from such DFT calculations if no additional investigations are carried out. The diopside structure has six different defect combinations with the first next nearest distance between M1 and T

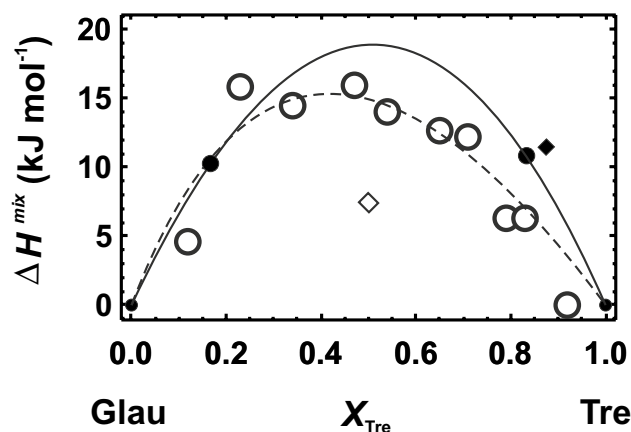


Fig. 8 Heat of mixing (ΔH^{mix}) of the glaucophane (Glau)–tremolite (Tre) solid solution. Open circles represent the enthalpy data derived from the correlation between $\delta\Delta_{\text{corr}}$ and ΔH^{mix} of Etzel and Benisek (2008) using the $\delta\Delta_{\text{corr}}$ data of Jenkins et al. (2014) from the low wavenumber region. Solid line and solid circles represent the data from the single defect method (LDA) of this study (using the two first next nearest defect pairs). Closed diamond represents a value obtained by using one of the four second next nearest defect combinations. Open diamond is the DFT calculated ΔH^{mix} of a fully ordered solid solution. Broken line is from Jenkins et al. (2014)

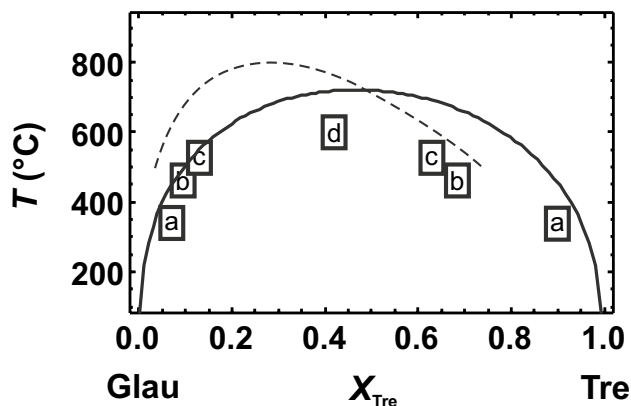


Fig. 9 Miscibility gap of the glaucophane (Glau)–tremolite (Tre) join at ~ 1.8 GPa. Solid line represents the results derived from the calculated enthalpy, entropy and volume data of this study. Open rectangles represent data based on coexisting natural amphiboles from a Black (1973), b Schliestedt (1980), c Reynard and Balleve (1988) and d Maresch et al. (1982). Broken line was taken from Jenkins et al. (2014)

(~3.3 Å). Because of this relatively large number of combinations, no DFT computations on structures with defect pairs having larger distances were performed.

Tremolite–glaucophane solid solution

Amphiboles have four different M sites. In tremolite, M4 is occupied by Ca and the other M positions by Mg. In glaucophane, M4 is occupied by Na, Al is fully ordered on the

adjacent M2 site for temperatures lower than 1000 K (e.g. Papike and Clark 1968; Palin et al. 2003), and the other M sites are occupied by Mg. Such a highly Al-ordered state is, however, only present in alkali amphiboles because of its monovalent M4 cation. On the other hand, in calcic amphiboles, Al is highly disordered over the M2 and M3 sites (Palin et al. 2003). For the sake of simplicity, the glaucophane defect in the tremolite-rich phase was constructed by positioning Na on M4 and Al only on M2. The tremolite defect in the

Table 1 Excess thermodynamic properties of the investigated binaries

	Observed	DFT-calculated				a^{id}	
	$\max \Delta H^{mix}$ (kJ/mol)	$\max \Delta H^{mix}$ (kJ/mol)	W_{AB}^H (kJ/mol)	W_{BA}^H (kJ/mol)	$W_{AB}^{\delta vib}$ (J/mol/K)		$W_{BA}^{\delta vib}$ (J/mol/K)
NaCl–KCl	4.5 ^b	4.75 ^a	16.45 ^a	22.01 ^a	8.73 ^c	8.73 ^c	$a_{NaCl}^{id} = X_{Na}$ $a_{KCl}^{id} = X_{K}$
Pyrope–grossular (Py–Gr)	9.6 ^d	9.3 ^a	32.72 ^a	44.50 ^a	–7.4 ^e	27.9 ^e	$a_{Py}^{id} = X_{Mg}^3$ $a_{Gr}^{id} = X_{Ca}^3$
MgO–CaO	–	19.2 ^a	65.24 ^a	86.84 ^a	10.8 ^a	10.8 ^a	$a_{MgO}^{id} = X_{Mg}$ $a_{CaO}^{id} = X_{Ca}$
Low albite– microcline (Ab– Mic)	8.1 ^f	6.5 ^a	20.59 ^a	31.30 ^a	9.1 ^g	9.1 ^g	$a_{Ab}^{id} = X_{Na}$ $a_{Mic}^{id} = X_{K}$
Diopside–jadeite (Di–Jd)	7.8 ^h	7.0 ^a	27.98 ^a	27.98 ^a	2.54 ⁱ	2.54 ⁱ	$a_{Di}^{id} = X_{Ca}^{M2} X_{Mg}^{M1}$ $a_{Jd}^{id} = X_{Na}^{M2} X_{Al}^{M1}$ $T > 1350 \text{ K}^n$
Diopside–CaTs (Di–CaTs)	6.0 ^k	6.0 ^j	7.70 ^j	37.44 ^j	0 ^l	0 ^l	$a_{Di}^{id} = X_{Mg}^{M1} (X_{Si}^T)^2$ $a_{CaTs}^{id} = 4X_{Al}^{M1} X_{Al}^T X_{Si}^T + SRO^o$
Glaucophane– tremolite (Glauc–Tre)	16.0 ^m	18.5 ^a	78.58 ^a	72.91 ^a	11.73 ⁱ	11.73 ⁱ	$a_{Glauc}^{id} = (X_{Na}^{M4})^2 (X_{Al}^{M2})^2$ $a_{Tre}^{id} = (X_{Ca}^{M4})^2 (X_{Mg}^{M2})^2 + SRO^p$

$\max \Delta H^{mix}$ is the heat of mixing at the mole fraction where it is at its maximum. DFT-derived values are compared to observed ones. W_{AB}^H and W_{BA}^H are the enthalpic interaction parameters of the asymmetric Margules mixing model, $\Delta H^{mix} = (1 - X_B) X_B^2 W_{AB}^H + (1 - X_B)^2 X_B W_{BA}^H$, of the A–B binary. $W_{AB}^{\delta vib}$ and $W_{BA}^{\delta vib}$ are the interaction parameters for the vibrational excess entropy, $\Delta S_{vib}^{exc} = (1 - X_B) X_B^2 W_{AB}^{\delta vib} + (1 - X_B)^2 X_B W_{BA}^{\delta vib}$. To calculate the excess Gibbs energy of mixing, use $W^G = W^H - T W^{\delta}$ and $G^{exc} = (1 - X_B) X_B^2 W_{AB}^G + (1 - X_B)^2 X_B W_{BA}^G$. Ideal mixing is defined in the last column (a^{id}). To define the solvus, the use of a configurational excess entropy is needed in most cases, which is, however, not listed because it is only valid at the solvus temperatures and may vanish at higher temperatures

^aDFT methods using LDA functional, this study

^bSolution calorimetry (Barrett and Wallace 1954)

^cLow-temperature calorimetry (Benisek and Dachs 2013)

^dSolution calorimetry (Newton et al. 1977)

^eLow-temperature calorimetry (Dachs 2006)

^fSolution calorimetry (Hovis 2017)

^gLow-temperature calorimetry (Benisek et al. 2014)

^hSolution calorimetry (Wood et al. 1980)

ⁱAccording to Benisek and Dachs (2012)

^jDFT methods using a partly disordered CaTs endmember

^kSolution calorimetry (Newton et al. 1977; Benisek et al. 2007)

^lLow-temperature calorimetry (Etzel et al. 2007)

^mDerived from line broadening in IR according to Etzel and Benisek (2008)

ⁿAt $T < 1350 \text{ K}$, short-range ordering is present and at $T < 1000 \text{ K}$, long-range ordering exists (Fleet et al. 1978)

^oShort-range ordering is present; see for example Benisek et al. (2007)

^pPossible short-range ordering is present, this study

glaucophane-rich phase consisted of Ca on M4 and Mg on M2. There are two defect combinations with the first next nearest M4–M2 distance and four combinations with the second next nearest distance. The latter yielded slightly larger ΔH^{mix} values than the former. The first next nearest combinations were described by a Margules mixing model using $W^H_{\text{TreGla}} = 72.91$ kJ/mol and $W^H_{\text{GlaTre}} = 78.58$ kJ/mol. This ΔH^{mix} behaviour is plotted in Fig. 8, where it is compared with enthalpic data obtained from the relation between line broadening in IR spectra ($\delta\Delta\text{corr}$) and ΔH^{mix} according to Etzel and Benisek (2008) using the $\delta\Delta\text{corr}$ data of Jenkins et al. (2014). Figure 8 also shows the ΔH^{mix} behaviour from Jenkins et al. (2014) derived from phase equilibrium experiments performed on the miscibility gap. Jenkins et al. (2014) also investigated $\delta\Delta\text{corr}$ of their synthetic samples and used these values to extract ΔH^{mix} after Etzel and Benisek (2008). They obtained maximum values of 14 kJ/mol, if $\delta\Delta\text{corr}$ is taken from the low wavenumber region, corresponding to a symmetrical W_{TreGla} of 56 kJ/mol (based on $\Delta H^{\text{mix}} = X_{\text{Tre}}X_{\text{Gla}}W_{\text{TreGla}}$ and $X_{\text{Tre}} = X_{\text{Gla}} = 0.5$). Their experimentally derived $W_{\text{TreGla}} = 70$ kJ/mol leads to a solvus with an apex of around 800 °C (Jenkins et al. 2014, their Fig. 4). The statement of Jenkins et al. (2014, p. 739) that a maximum $\Delta H^{\text{mix}} = 14$ kJ/mol would lead to an unrealistically high critical temperature of the solvus (~4000 °C) is obviously wrong.

The DFT calculations yielded slightly larger ΔH^{mix} values than the data derived from $\delta\Delta\text{corr}$ and from the phase equilibrium experiments (Fig. 8). To calculate the solvus, $\Delta S_{\text{vib}}^{\text{exc}}$ was again calculated according to Benisek and Dachs (2012), yielding $W_{\text{vib}}^S = 11.73$ J/mol/K. The configurational entropy was calculated assuming mixing on four sites. The resulting solvus is shown in Fig. 9, where it is compared to the solvus from Jenkins et al. (2014) and coexisting natural amphiboles. The solvus based on the DFT calculations shows a similar height, but an asymmetry that does not agree with the natural and experimental evidence. This result is most likely a consequence of the assumed simple model for the configurational entropy. In the tremolite-rich region, Al may also occupy the M3 site, increasing the configurational entropy, whereas the glaucophane-rich region may be characterised by a stricter ordering not correctly described by mixing on four sites.

Conclusions

The DFT-calculated mixing properties of all investigated solid solutions are summarised and, if possible, compared with measured ones in Table 1. This study showed that DFT calculations in combination with the single defect method can generate accurate heat of mixing values, amazingly accurate for simple solid solutions. This method allows the investigation of this property considerably faster than

calorimetric methods (the DFT calculations are performed within weeks compared to years for calorimetric work). In cases where ordering effects play a dominant role (mixing on two different crystallographic sites), additional information is needed to predict valuable results. If this method can be expanded to binary systems containing Fe remains the subject of further studies and is tested presently.

Acknowledgements Open access funding provided by Austrian Science Fund (FWF). This work was supported by grants from the Austrian Science Fund (FWF), Project Number P 28724, which is gratefully acknowledged. We thank E. Forsthofer for his professional work in implementing and maintaining the Materials Studio software at the Salzburg University. We also thank the two anonymous reviewers, whose comments were very helpful in improving the manuscript.

Open Access This article is licensed under a Creative Commons Attribution 4.0 International License, which permits use, sharing, adaptation, distribution and reproduction in any medium or format, as long as you give appropriate credit to the original author(s) and the source, provide a link to the Creative Commons licence, and indicate if changes were made. The images or other third party material in this article are included in the article's Creative Commons licence, unless indicated otherwise in a credit line to the material. If material is not included in the article's Creative Commons licence and your intended use is not permitted by statutory regulation or exceeds the permitted use, you will need to obtain permission directly from the copyright holder. To view a copy of this licence, visit <http://creativecommons.org/licenses/by/4.0/>.

References

- Bachinski SW, Müller G (1971) Experimental determinations of the microcline–low albite solvus. *J Petrol* 12:329–356
- Barrett WT, Wallace WE (1954) Studies of NaCl–KCl solid solutions. I. Heats of formation, lattice spacings, densities, Schottky defects and mutual solubilities. *J Am Chem Soc* 76:366–369
- Benisek A, Dachs E (2012) A relationship to estimate the excess entropy of mixing: application in silicate solid solutions and binary alloys. *J Alloys Compd* 527:127–131
- Benisek A, Dachs E (2013) Calorimetric study of the entropy relation in the NaCl–KCl system. *J Chem Thermodyn* 62:231–235
- Benisek A, Dachs E (2018) The accuracy of standard enthalpies and entropies for phases of petrological interest derived from density-functional calculations. *Contrib Mineral Petrol* 173:90
- Benisek A, Kroll H, Cemic L, Kohl V, Breit U, Heying B (2003) Enthalpies in (Na, Ca)- and (K, Ca)-feldspar binaries: a high-temperature solution calorimetric study. *Contrib Mineral Petrol* 145:119–129
- Benisek A, Etzel K, Cemic L (2007) Thermodynamic mixing behaviour of synthetic Ca-Tschemak-diopside pyroxene solid solutions: II. Heat of mixing and activity-composition relationships. *Phys Chem Miner* 34:747–755
- Benisek A, Dachs E, Kroll H (2014) Thermochemistry of the alkali feldspars: calorimetric study of the entropy relations in the low albite–low microcline series. *Am Mineral* 99:76–83
- Benisek A, Dachs E, Grodzicki M (2018) Vibrational entropy of disorder in Cu_3Au with different degrees of short-range order. *Phys Chem Chem Phys* 20:19441
- Black PM (1973) Mineralogy of New Caledonian metamorphic rocks II. Amphiboles from the Ouegoa district. *Contrib Mineral Petrol* 39:55–64

- Bosenick A, Dove MT, Warren MC, Fischer A (1999) Local cation distribution of diopside–Ca–Tschermak solid solutions: a computational and ^{29}Si MAS NMR spectroscopic study. *Eur J Mineral* 9:39
- Carpenter MA, McConnell JDC, Navrotsky A (1985) Enthalpies of ordering in the plagioclase feldspar solid solution. *Geochim Cosmochim Acta* 49:947–966
- Ceperley DM, Alder BJ (1980) Ground state of the electron gas by a stochastic method. *Phys Rev Lett* 45:566–569
- Clark SJ, Segall MD, Pickard CJ, Hasnip PJ, Probert MIJ, Refson K, Payne MC (2005) First principles methods using CASTEP. *Z Kristallogr* 220:567–570
- Cohen RE (1985) Thermodynamics aluminous pyroxenes: effects of short-range order. Ph.D. dissertation, Harvard University
- Dachs E (2006) Heat capacities and entropies of mixing of pyrope-grossular ($\text{Mg}_3\text{Al}_2\text{Si}_3\text{O}_{12}$ – $\text{Ca}_3\text{Al}_2\text{Si}_3\text{O}_{12}$) garnet solid solutions: a low-temperature calorimetric and a thermodynamic investigation. *Am Mineral* 91(5–6):894–906
- Dachs E, Benisek A (2019) A new activity model for Mg–Al biotites determined through an integrated approach. *Contrib Mineral Petrol* 174:76
- Doman RC, Barr JB, McNally RN, Alper AM (1963) Phase equilibria in the system CaO–MgO. *J Am Ceram Soc* 46:313–316
- Etzel K, Benisek A (2008) Thermodynamic mixing behaviour of synthetic Ca–Tschermak–diopside pyroxene solid solutions: III. An analyses of IR line broadening and heat of mixing behaviour. *Phys Chem Miner* 35:399–407
- Etzel K, Benisek A, Dachs E, Cemič L (2007) Thermodynamic mixing behavior of synthetic Ca–Tschermak–diopside pyroxene solid solutions: I. Volume and heat capacity of mixing. *Phys Chem Miner* 34(10):733–746
- Fleet ME, Herzberg CT, Bancroft GM, Aldridge LP (1978) Omphacite studies; I, The P2/nC2/c transformation. *Am Mineral* 63:1100–1106
- Fleming RL, Luth RW (2002) ^{29}Si MAS NMR study of diopside–Ca–Tschermak clinopyroxenes: detecting both tetrahedral and octahedral Al substitution. *Am Mineral* 87:25–36
- Gasparik T (1985) Experimentally determined compositions of diopside–jadeite pyroxene in equilibrium with albite and quartz at 1200–1350 °C and 15–34 kbar. *Geochim Cosmochim Acta* 49:865–870
- Geiger CA (2001) Thermodynamic mixing properties of binary oxide and silicate solid solutions determined by direct measurements: the role of strain. In: Geiger CA (ed) *Solid solutions in silicate and oxide systems*, EMU notes in mineralogy, vol 3. Eötvös University Press, Budapest, pp 71–96
- Haselton HT Jr, Hovis GL, Hemingway BS, Robie RA (1983) Calorimetric investigation of the excess entropy of mixing in analbite–sanidine solid solutions: lack of evidence for Na, K short-range order and implications for two-feldspar thermometry. *Am Mineral* 68:398–413
- Hovis GL (1988) Enthalpies and volumes related to K–Na mixing and Al–Si order/disorder in alkali feldspars. *J Petrol* 29:731–763
- Hovis GL (2017) A refined view of the thermodynamic mixing quantities for alkali feldspars and the quandary of excess configurational entropy. *Am J Sci* 317:597–640
- Jenkins DM, Carpenter MA, Zhang M (2014) Experimental and infrared characterization of the miscibility gap along the tremolite–glaucofane join. *Am Mineral* 99:730–741
- Li Y, Kowalski PM, Blanca-Romero A, Vinograd V, Bosbach D (2014) Ab initio calculation of excess properties of $\text{La}_{1-x}(\text{Ln}, \text{M})_x\text{PO}_4$ solid solutions. *J Solid State Chem* 220:137–141
- Maresch WV, Medenbach O, Rudolph A (1982) Winchite and the actinolite–glaucofane miscibility gap. *Nature* 296:731
- Monkhorst HJ, Pack JD (1976) On special points for Brillouin zone integrations. *Phys Rev B* 13:5188
- Navrotsky A (1997) Progress and new directions in high temperature calorimetry revisited. *Phys Chem Miner* 24:222–241
- Newton RC, Charlu TV, Kleppa OJ (1977) Thermochemistry of high pressure garnets and clinopyroxenes in the system CaO–MgO– Al_2O_3 – SiO_2 . *Geochim Cosmochim Acta* 41:369–377
- Ozolins V, Wolverson C, Zunger A (1997) Cu–Au, Ag–Au, Cu–Ag and Ni–Au intermetallics: first-principles study of phase diagrams and structures. *Phys Rev B* 57:6427
- Palin EJ, Guiton BS, Craig MS, Welch MD, Dove MT, Redfern SAT (2003) Computer simulation of Al–Mg ordering in glaucophane and a comparison with infrared spectroscopy. *Eur J Mineral* 15:893–901
- Papike JJ, Clark JR (1968) The crystal structure and cation distribution of glaucophane. *Am Mineral* 53:1156–1173
- Perdew JP, Burke K, Ernzerhof M (1996) Generalized gradient approximation made simple. *Phys Rev Lett* 77:3865–3868
- Perdew JP, Ruzsinszky A, Csonka GI, Vydrov OA, Scuseria GE, Constantin LA, Zhou X, Burke K (2008) Restoring the density-gradient expansion for exchange in solids and surfaces. *Phys Rev Lett* 100:136406
- Pfrommer BG, Cote M, Louie SG, Cohen ML (1997) Relaxation of crystals with the quasi-Newton method. *J Comput Phys* 131:233–240
- Reynard B, Ballevre M (1988) Coexisting amphiboles in an eclogite from the Western Alps: new constraints on the miscibility gap between sodic and calcic amphiboles. *J Metamorph Geol* 6:333–350
- Schliestedt M (1980) Phasengleichgewichte in Hochdruckgesteinen von Sifnos, Griechenland. Unpublished Dissertation, University of Braunschweig
- Sluiter MHF, Kawazoe Y (2002) Prediction of the mixing enthalpy of alloys. *Europhys Lett* 57:526–532
- Sluiter MHF, Vinograd V, Kawazoe Y (2004) Intermixing tendencies in garnets: pyrope and grossular. *Phys Rev B* 70:184120
- Vesnin YI, Zakovryashin SP (1979) About the decay of solid solutions KCl–NaCl. *Solid State Commun* 31:635–640
- Vinograd VL, Sluiter MHF (2006) Thermodynamics of mixing in pyrope–grossular, $\text{Mg}_3\text{Al}_2\text{Si}_3\text{O}_{12}$ – $\text{Ca}_3\text{Al}_2\text{Si}_3\text{O}_{12}$, solid solution from lattice dynamics calculations and Monte Carlo simulations. *Am Mineral* 91:1815–1830
- Vinograd VL, Winkler B (2010) An efficient cluster expansion method for binary solid solutions: application to the halite–sylvite, NaCl–KCl, system. *Rev Mineral Geochem* 71:413–436
- Vinograd VL, Gale JD, Winkler B (2007) Thermodynamics of mixing in diopside–jadeite $\text{CaMgSi}_2\text{O}_6$ – $\text{NaAlSi}_2\text{O}_6$, solid solution from static lattice energy calculations. *Phys Chem Miner* 34:713–725
- Vinograd VL, Sluiter MHF, Winkler B (2009) Subsolidus phase relations in the CaCO_3 – MgCO_3 system predicted from the excess enthalpies of supercell structures with single and double defects. *Phys Rev B* 79:104201
- Vinograd VL, Brandt F, Rozov K, Klinkenberg M, Refson K, Winkler B, Bosbach D (2013) Solid–aqueous equilibrium in the BaSO_4 – RaSO_4 – H_2O system: first-principles calculations and a thermodynamic assessment. *Geochim Cosmochim Acta* 122:398–417
- Vinograd VL, Kulik DA, Brandt F, Klinkenberg M, Weber J, Winkler B, Bosbach D (2018) Thermodynamics of the solid solution–aqueous solution system $(\text{Ba}, \text{Sr}, \text{Ra})\text{SO}_4 + \text{H}_2\text{O}$: I. The effect of strontium content on radium uptake by barite. *Appl Geochem* 89:59–74
- Wood BJ, Holland TJB, Newton RC, Kleppa OJ (1980) Thermochemistry of jadeite–diopside pyroxenes. *Geochim Cosmochim Acta* 44:1363–1371
- Yin Y, Argent BJB (1993) The phase diagrams and thermodynamics of the ZrO_2 –CaO–MgO and MgO–CaO systems. *J Phase Equilib* 14:588–600